

Comparative simulation of DC and AC performances of $\text{Al}_{0.26}\text{Ga}_{0.74}\text{N}/\text{GaN}$ HEMT with B GaN Back Barrier

Imane Four^{1*}, Mohammed Kameche²

¹ STIC Laboratory, Abou-bekr Belkaid University of Tlemcen, Algeria

² The Satellite Development Centre Oran, Algeria

Received 29 August 2020, Revised 3 December 2020, Accepted 7 December 2020

ABSTRACT

This paper discusses the influence of B GaN layer on the structure of $\text{Al}_{0.26}\text{Ga}_{0.74}\text{N}/\text{B}_{0.02}\text{Ga}_{0.98}\text{N}/\text{GaN}$ HEMT with T- Gate. The use of B GaN back barrier on this device enhances confinement of the electron in the device. We simulate DC and AC characteristics by using TCAD Silvaco. The obtained results shows a maximum drain current of 1 A/mm, a threshold voltage of -1.25 V, a maximum transconductance of 0.850 S mm⁻¹, an $I_{\text{ON}}/I_{\text{OFF}}$ ratio of 1.5×10^9 , a Drain Induced Barrier Lowering (DIBL) of 166 mV/V, a Sub-threshold Swing (SS) of 300 mV/dec and a Gate-leakage of 5.10^{-22} A. In terms of AC performances, the device offers Ft of 600 GHz and Fmax of 1 THz. These results revealed that the use of B GaN back barrier has added benefits in performance which can be an outstanding solution for high frequency switching and high-power applications.

Keywords: B GaN Back-Barrier, HEMT, DC performances, AC performances

1. INTRODUCTION

AlGaN /GaN High Electron Mobility Transistor (HEMT) has shown outstanding performances for a variety of high frequency and high-power applications. This is due to their exceptional material properties such as wide bandgap, high breakdown field and high electron saturation velocity [1]. The GaN-based microwave power devices and their relative devices have wide potential in the domain of satellite and radar communication [2].

Semiconductors' compound based on III-N materials such as GaN, AlN, BN and their alloys are direct gap semiconductors. These materials have emerged as materials of great interest in electronics and optoelectronics applications. In electronics, these materials are preferred manufacturer devices, having high power, high frequency and ability to operate at high temperature, such as field effect transistors and bipolar transistors, including transistors with high electron mobility [3].

Gallium-boron nitride (B GaN) is an alloy between boron nitride (BN) and gallium nitride (GaN). Boron nitride broadband prohibited films have drawn attention thanks to their remarkable properties such as thermal conductivity, hardness and excellent chemical stability. In addition, the network constants of the B GaN alloy can be adapted to those of SiC or AlN if enough incorporation of boron into the network is obtained [4]. Recently, the ternary B GaN was integrated in the conventional structure of the HEMT by Ougazzaden et al. [5] to ameliorate the performance by enhancing the confinement of carriers in the two-dimensional electron gas region [3]. In fact, Beghdadli et al. [6] have shown that electrical resistivity is strongly related to the incorporation of boron in B GaN alloys, while mobility increases up to 290 cm / Vs with increasing boron content up to at 1.75%. It can be said that a layer of B GaN can be very resistive with only a few percent of boron, which could be very interesting for devices such as HEMTs. In addition, there is an improvement of the resistivity followed by an increase of the mobility of the

* Corresponding Author: imane.four@univ-tlemcen.dz

carriers, thanks to the quality of good crystalline in the ternary BGaN [7]. The resistivity of the BGaN as a function of the boron fraction where a very substantial increase in the resistivity of $2.7 \times 10^{-2} \Omega \cdot \text{cm}$ is observed up to $7.4 \times 10^4 \Omega \cdot \text{cm}$ [6].

Recently, our first work [8] based on AlGaN /GaN HEMT without BGaN layer shows a good DC and RF characteristics. In order to benefit of the properties of BN, we will induce the ternary BGaN to improve the performance of AlGaN /GaN HEMT. In fact, this ternary can rise the GaN buffer resistivity and the electrons confinement when it is used.

In this work, we study the effect of BGaN back-barriers in AlGaN/GaN HEMT compared with the conventional HEMT used in [8]. The proposed structure consists of Si₃N₄ passivation layer which exhibits remarkable increase in drain current densities with a compromise of increased gate leakage [9], and minimizing the trap effects which influence the performance of HEMT [10]. Then, to improve the cutoff frequency of HEMT, there is a need to minimize the gate length (*L_g*) with respect to the aspect ratio *L_g/d_{gate}*-2DEG which be must sustained above 15 according to Jensen [11]. Afterward, to bring the problem of the disagreement mesh under control, these layers were grown on 4H-SiC substrate. 4H-SiC has the merit of small lattice mismatch to GaN epilayers, very high thermal conductivity and high resistivity [12]. Prominent literatures have demonstrated that the temperature in a GaN device growth on a 4H-SiC substrate is minimal compared to those fabricated on a sapphire substrate [13][14].

In this paper, we discuss the influence of the induction of BGaN ultrathin back barrier in AlGaN/GaN HEMT with T-gate based 4H-SiC substrate. It shows significant improvement in the DC and AC performances by ameliorating the efficiency of modulation of the electrons in the channel using TCAD Silvaco software. The layer of BGaN is very resistive with a few percent of boron, which is very interesting for devices such as HEMTs. Moreover, there will be improvement of the resistivity which increase the mobility of the carriers, because of the quality of good crystalline in the BGaN semiconductor. These results demonstrate the important of AlGaN/GaN/BGaN HEMT and indicate a splendid candidate for microwave and switching applications.

2. PROPOSED STRUCTURE AND SIMULATION MODEL

The structure of AlGaN/GaN/BGaN HEMT on 4H-SiC substrate was designed by using TCAD Silvaco software tool as presented in Fig. 1. The parameters of the proposed device structure are: Al_{0.26}Ga_{0.74}N Schottky layer with thickness of 24 nm, 35 nm n-type GaN channel layer, 8 nm B_{0.02}Ga_{0.98}N back-barrier and a 300 nm thick n-type GaN as buffer layer. Finally, the structure was passivated with 10 nm Si₃N₄ layer with 4H-SiC substrate.

This structure had T-shaped gold gate (work function 5.1 eV) of length (*L_G*) 30 nm. The source-gate (*L_{SG}*) and drain-gate (*L_{DG}*) distances are 0.681 μm and 0.1084 μm respectively. Length of Source (*L_S*) and Drain (*L_D*) is 0.5 μm. Table 1 shows the doping parameters of the structure.

Table 1. Doping parameter

Doping concentration	Value
GaN Cap doping n-concentration	$1 \cdot 10^{22}$ per cm^3
AlGaN layer doping n-concentration	$1 \cdot 10^{19}$ per cm^3
GaN channel doping n-concentration	$1 \cdot 10^{17}$ per cm^3
BGaN layer doping n-concentration	$1 \cdot 10^{16}$ per cm^3

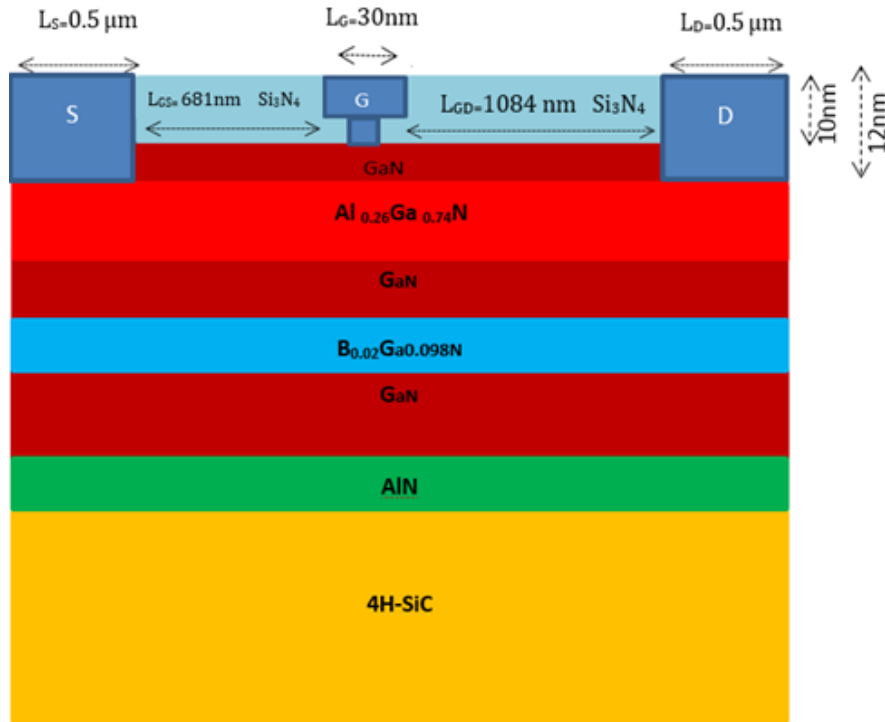


Figure 1. The structure of proposed HEMT.

In the ATLAS part of the input file, the contacts, materials and models are defined. For the GaN region, we declare the dependence of the mobility of the charge carriers on the doping; the recombination parameters (lifetime) are also applied. For AlN regions, the low field mobility and the lifetime of the charge carriers are explicitly specified in the material instruction. The new material $B_{0.02}Ga_{0.98}N$ and $Al_{0.26}Ga_{0.74}N$ are defined by a specific command [15]. The structure, designed using the DEVEDIT program can be seen in 2D as in Fig. 1. Basic parameters like electron affinity, lattice constant, density of states masses and permittivity are calculated by the following equations. Table 2 summarizes the values.

The lattice constant “a” of AlGaN can be calculated by linear interpolation [16]:

$$a(Al_xGa_{1-x}N) = xa(AlN) + (1 - x)a(GaN) \quad (1)$$

$$a(B_xGa_{1-x}N) = xa(BN) + (1 - x)a(GaN) \quad (2)$$

with $a(BN) = 0.253$ nm, $a(AlN) = 0.3112$ nm, and $a(GaN) = 0.3189$ nm.

The bandgap of AlGaN and B GaN are calculated from [16][17]:

$$E_G(Al_xGa_{1-x}N) = xE_G(AlN) + (1 - x)E_G(GaN) - 1.3x(1 - x) \quad (3)$$

$$E_G(B_xGa_{1-x}N) = xE_G(BN) + (1 - x)E_G(GaN) - 7.28x(1 - x) \quad (4)$$

with $E_G(GaN) = 3.415$ eV, $E_G(BN) = 5.8$ eV, and $E_G(AlN) = 6.15$ eV [1].

The affinity of electron is given by [17]:

$$\frac{\Delta EC}{\Delta EV} = \frac{0.7}{0.3} \quad (5)$$

The permittivity as a function of composition fraction x is given by [18]:

$$\epsilon(Al_xGa_{1-x}N) = 8.5x + 0.89(1 - x) \quad (6)$$

$$\epsilon(B_xGa_{1-x}N) = 8.5x + 0.89(1 - x) \quad (7)$$

The density of nitride of states masses [19]:

$$m_e (\text{Al}_x\text{Ga}_{1-x}\text{N}) = 0.314x + 0.2(1 - x), m_h (\text{Al}_x\text{Ga}_{1-x}\text{N}) = 0.417x + 1.0(1 - x) \quad (8)$$

$$m_e (\text{B}_x\text{Ga}_{1-x}\text{N}) = 0.35x + 0.2(1 - x), m_h (\text{Al}_x\text{Ga}_{1-x}\text{N}) = 0.37x + 1.0(1 - x) \quad (9)$$

TABLE 2. Simulation parameter

Parameter	GaN	AlN	B _{0.02} Ga _{0.96} N	Al _{0.26} Ga _{0.74} N	4H-SiC
E_g(eV)	3.43	6.13	3.33	3.88	3.36
χ(cm²/vs)	4.1	2.2	4.16	3.78	3.24
N_c(cm⁻³)	2.24	4.41 10 ¹⁸	2.29 10 ¹⁸	2.75 10 ¹⁸	1.2310 ¹⁹
N_v(cm⁻³)	2.5 10 ¹⁹	6.75 10 ¹⁸	2.46 10 ¹⁹	1.95 10 ¹⁹	4.5810 ¹⁸
ε	8.9	8.5	8.86	8.79	6.63

3. RESULTS AND DISCUSSION

3.1 DC PERFORMANCES

The principal function of HEMT can be explained by the band diagram of energy. It presents the conduction and valence band energies as a function of depth from surface along the vertical direction of the device AlGa_n/B_{0.02}Ga_{0.98}N/GaN and AlGa_n/Ga_n as shown in Fig. 2.

The juxtaposition of a large gap material (AlGa_n) with a small gap material (Ga_n) implies the creation a discontinuity on the conduction band at the interface of the two materials AlGa_n and Ga_n and this is called heterojunction.

This heterojunction induces the creation of a potential well which is indicated by the circle No. 1, in both structures of without and with B_{0.02}Ga_{0.98}N back barrier where the two-dimensional gas (2DEG) is created. Electrons are transmitted and cumulated in this well. Besides, there is an increase in the conduction band as well as the formation of an energy peak which is indicated by circle No. 2 in HEMT with B_{0.02}Ga_{0.98}N back barrier. The peak is an electrostatic barrier that opposes the electrons migration from the potential well, which makes the escape of electrons from this well more difficult.

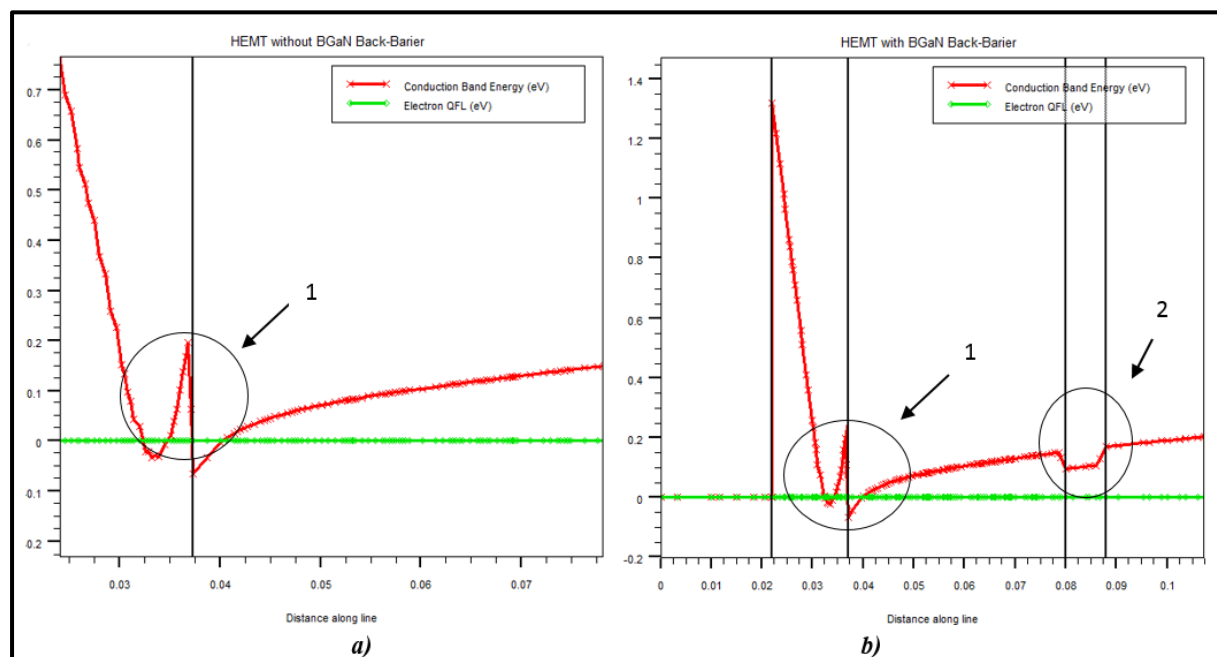


Figure 2. Band diagram of energy a) $\text{Al}_{0.26}\text{Ga}_{0.74}\text{N} / \text{GaN}$ HEMT, b) $\text{Al}_{0.26}\text{Ga}_{0.74}\text{N} / \text{B}_{0.02}\text{Ga}_{0.98}\text{N} / \text{GaN}$ HEMT

Fig. 3 presents the output characteristics ($I_{\text{DS}} - V_{\text{DS}}$) where the I_{DS} current flowing between the drain and the source were calculated by varying the V_{DS} voltage from 0 V to 10 V, for different values of gate-source control voltage (V_{GS}) from 0 V to -2 V. The result exhibits the maximum drain current obtained as 1A/mm for the device with back barrier which is better than the 0.6 A /mm acquired from the structure without back barrier [8].

The ($I_{\text{DS}} - V_{\text{DS}}$) characteristics display a good pinch voltage. This demonstrates that the electrons are well confined with the BGeN back barrier layer.

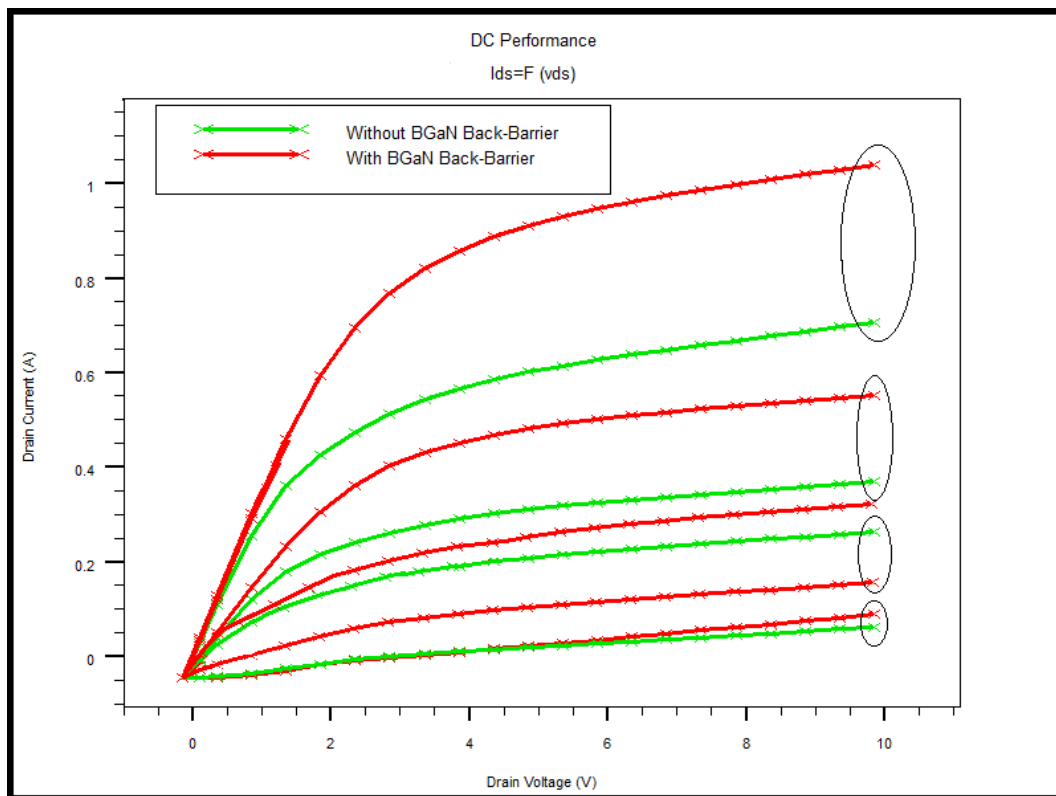


Figure 3. $I_{\text{DS}} - V_{\text{DS}}$ characteristics while V_{GS} is swept from 0.0 V to -2 V.

Fig. 4 shows the transfer characteristics which represents the evolution of the drain-source current (I_{DS}) as a function of the gate-source voltage for a constant drain-source voltage at 1.0 V. The threshold voltage V_{th} is about -1.5 V for the structure with BGeN back barrier, which is lower than the value achieved of -3.5 V for HEMT without BGeN back barrier.

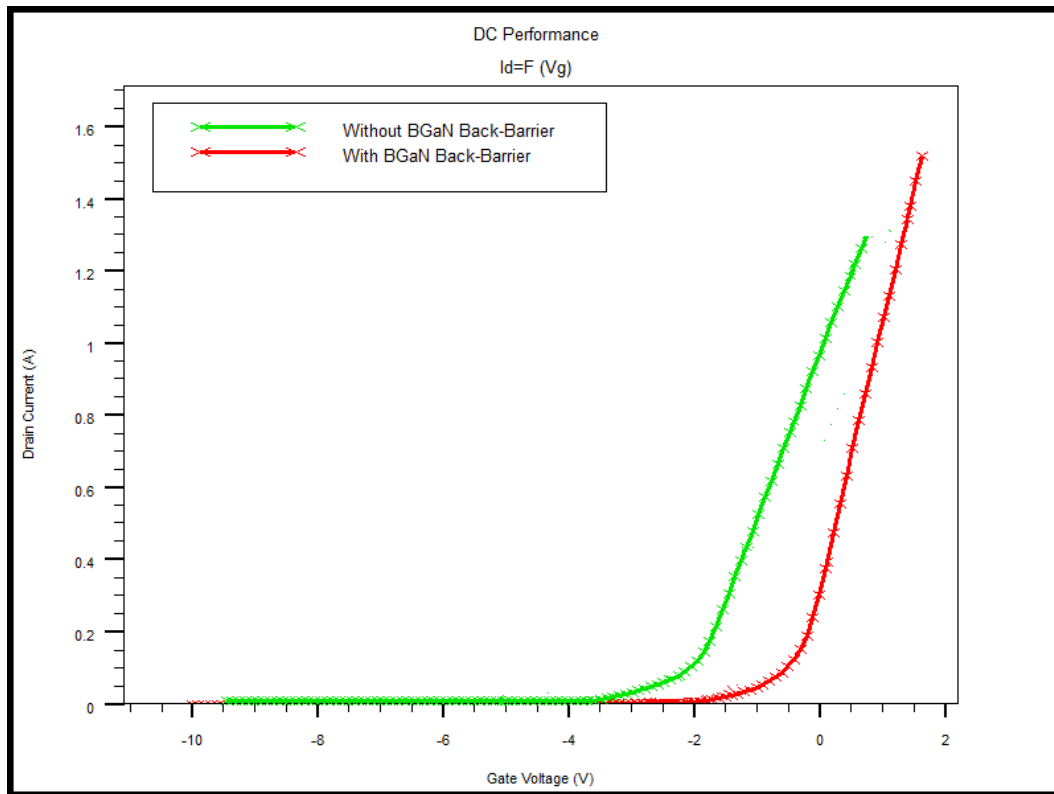


Figure 4. (I_{DS} - V_{GS}) characteristics with $V_{ds} = 1.0$ V.

The variation of the transconductance (G_m) is presented in Fig. 5. The simulation displays a maximum transconductance of 850 mS/mm at $V_G = -1.0$ V for the structure with B GaN back barrier, which is better than 200 mS/mm obtained for the HEMT without B GaN back barrier.

The curve of the simulated structure is explained by a strong concentration of electrons available for conduction as we all know that boron is resistive [5]. Consequently, when we make 2% of the concentration of boron, the resistivity of the electrostatic barrier increases in same time with increment of the mobility of the electrons, which improves the electron confinement and directly increases the I_{DS} output current, and since the transconductance is proportional to the I_{DS} current, G_m also increases.

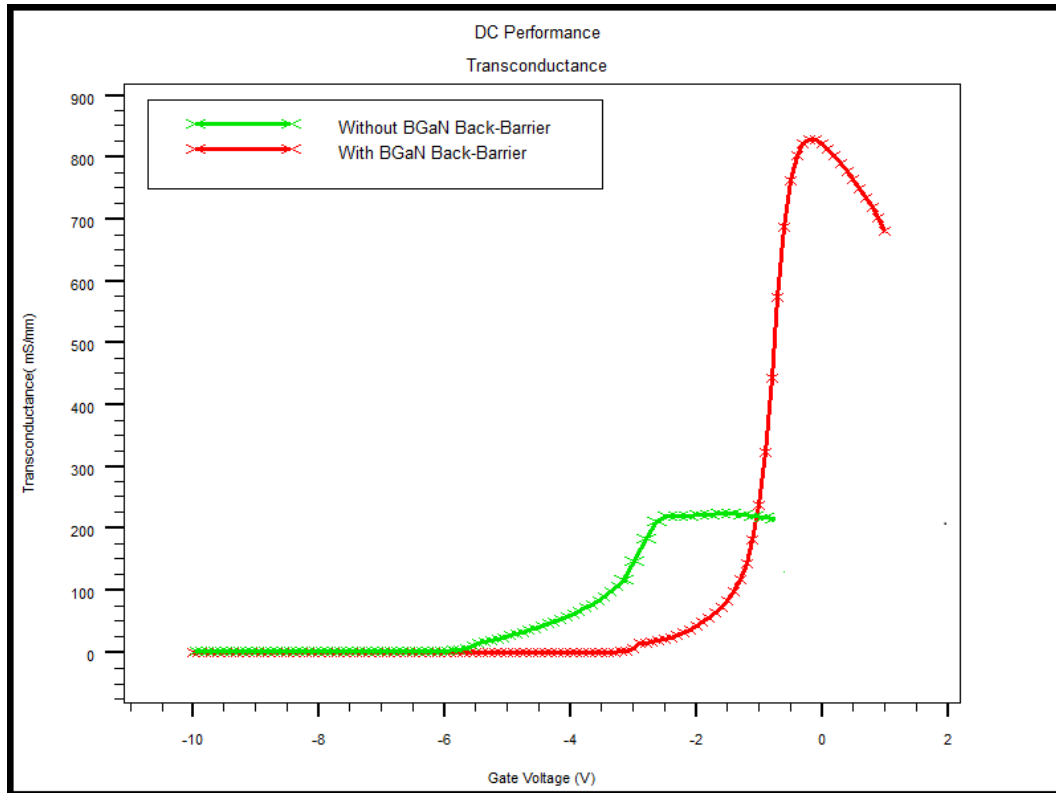


Figure 5. Transconductance (G_m) versus (V_{GS})

Fig. 6 shows the Sub-threshold Swing, SS which is determined from the log characteristic (I_{DS}) versus V_{GS} . It corresponds to the gate-source voltage applied to reduce the drain current. The curve is on a logarithmic scale, where,

$$SS = \text{Abs} [V_{GS2} - V_{GS1}] \quad [8] \quad (10)$$

The sub-threshold slope is therefore equal to 300 mV / dec. So, the HEMT with BGaN back barrier presents better Sub-threshold Swing compared the structure without BGaN back barrier which was 200 mV/dec [8].

We can also bring out the I_{ON} and the I_{OFF} to calculate the I_{ON}/I_{OFF} ratio.

The $I_{ON} = 9.10^0$ and $I_{OFF} = 6.10^{-9}$, resulting in an I_{ON}/I_{OFF} ratio of $1.5 \cdot 10^9$. A large I_{ON}/I_{OFF} ratio indicates the quality of the device, in other words a low loss.

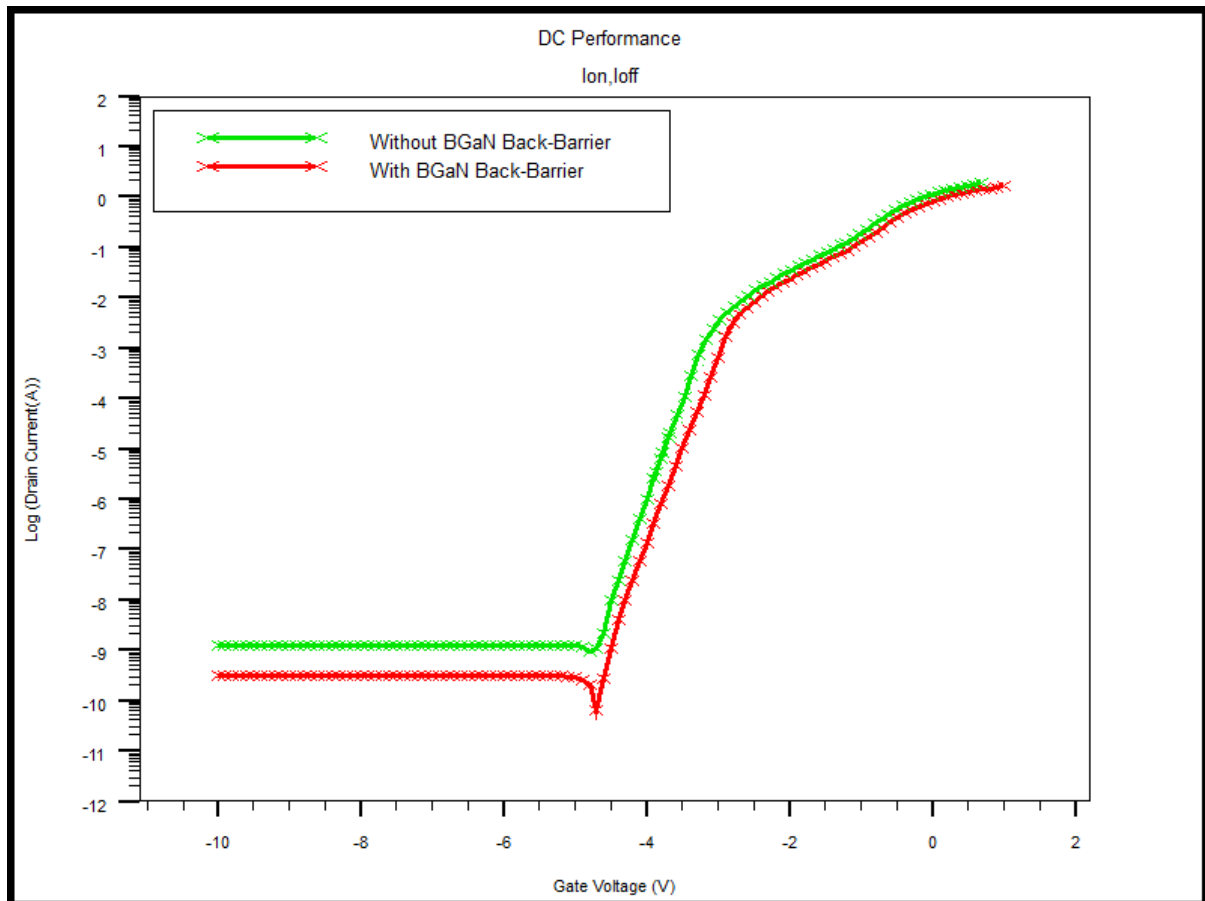


Figure 6. Logarithmic plots of (I_{DS} - V_{GS})

Fig. 7 is used to determine the leakage current at the gate level. We have a very low minimum leakage current equal to 5×10^{-22} A at $V_{GS} = 0$ V, and a maximum leakage current of 5×10^{-20} A. The leakage of current is a consequence of the trapping effects, the surface, and the short channel effects (SCE). Therefore, the leakage of electron reduces the output current. These are excellent values to minimize the consumption.

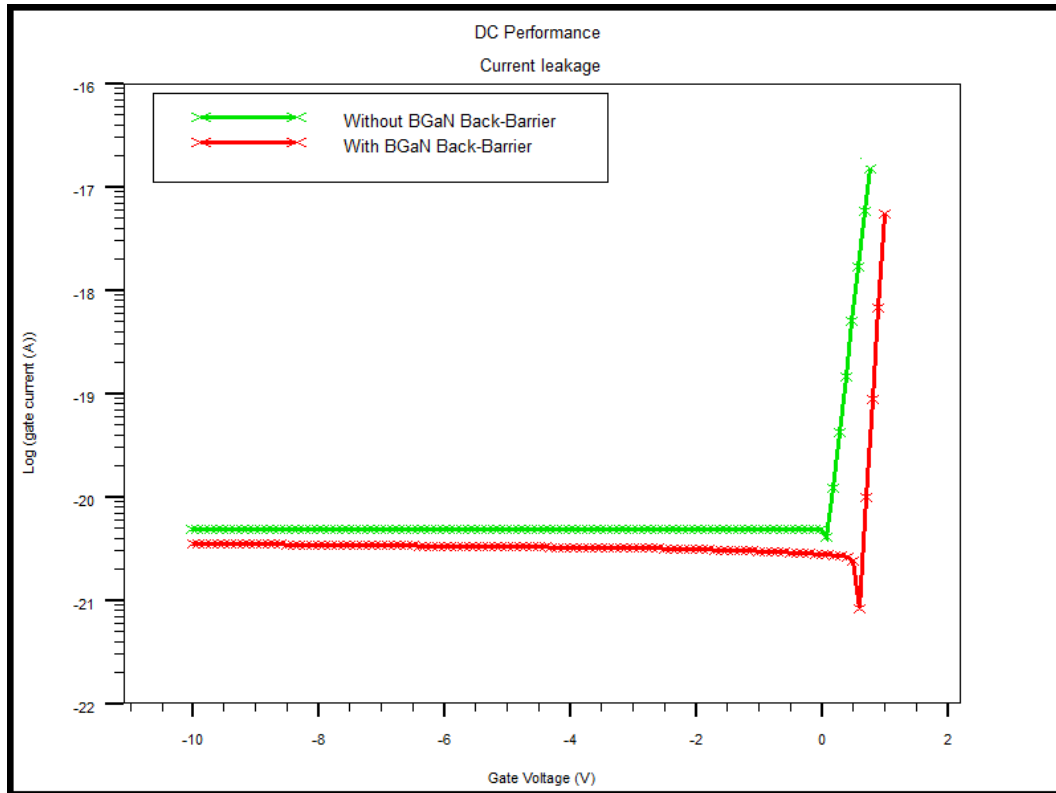


Figure 7. Leakage current of the gate

DIBL (Drain Induced Barrier Lowering) is a more important phenomenon for high drain voltages in short channel transistors and is mainly used for digital applications. It can be determined using Eq. 12.

We calculate the threshold voltage V_{TH} for two different values of V_{DS} at 5 V and 8 V. The curves are shown in Fig. 8.

The values extracted from the program with B GaN back barrier are: $V_{TH} = -2.5$ V for $V_{DS} = 8$ V (green curve), and $V_{TH} = -2.8$ V for $V_{DS} = 16$ V (red curve).

$$DIBL = \text{Abs} [\Delta V_{TH} / \Delta V_{DS}] [8] \quad (12)$$

The DIBL is 166 mV / V; it is a very good value and better than 22 mV / V as showed in structure of HEMT without B GaN back barrier.

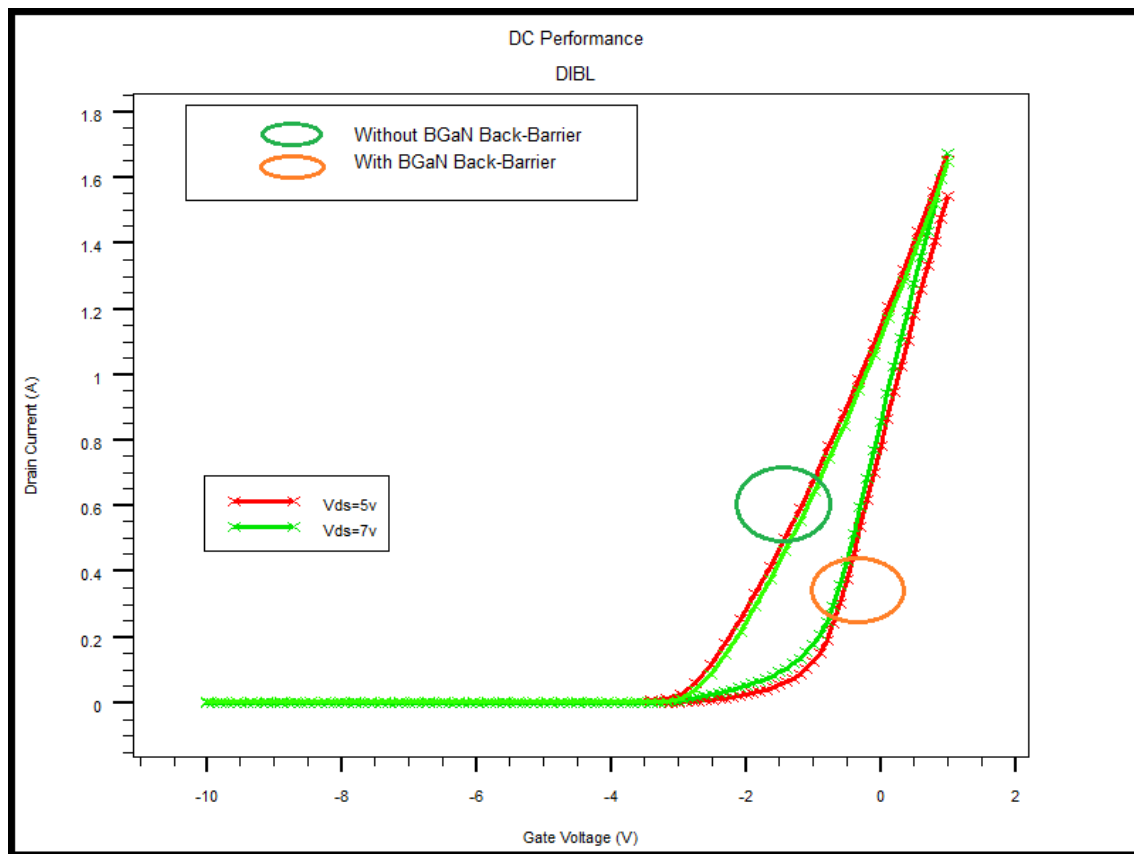


Figure 8. (I_{ds} - V_{gs}) while $V_{DS} = 5.0$ V and 7.0 V.

3.2 AC PERFORMANCES

Fig. 9 illustrates two important characteristics in HEMT: the transition frequency (F_t) which is the frequency when the module of the current gain is equal to 1 A, and the maximum oscillation frequency (F_{max}) for which the gain in power is equal to 1. The simulation was made at $V_{GS} = 0$ V. The result shows a cutoff frequency equal to 600 GHz and a maximum oscillation frequency F_{max} equal to 1THz for the structure with BGaN back barrier. For the HEMT without BGaN back barrier, the cut-off frequency is 50 GHz and the maximum oscillation frequency is approximately of 150 GHz.

We obtain improved frequencies by inducing $B_{0.02}Ga_{0.98}N$, which rises the resistivity of the buffer. It enhances the electron confinement and concentration at the AlGa_N/Ga_N interface. The result obtained is outstanding compared with the first work done without BGaN back barrier [8].

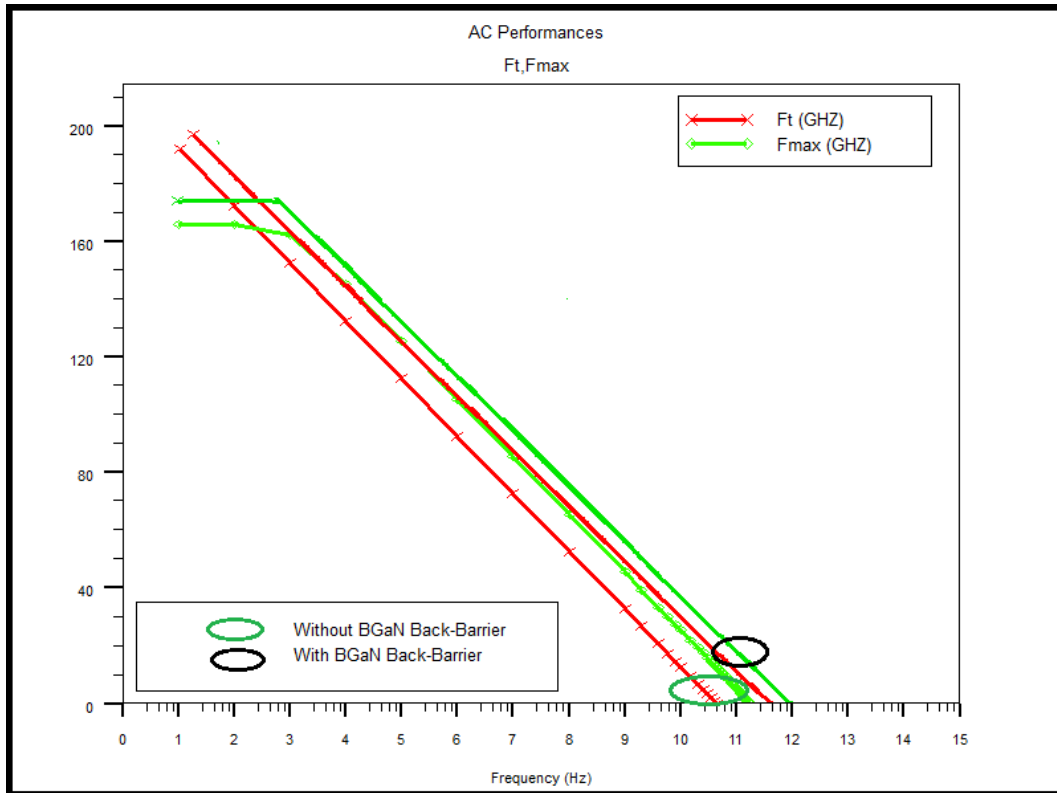


Figure 9. The transition frequency (Ft) and the frequency of maximum oscillation (Fmax) at $V_{DS} = 5.0 \text{ V}$ / $V_{GS} = 1.0 \text{ V}$.

Fig. 10 shows stable maximum power gain (GMS) and available maximum power gain (GMA) for $V_{DS} = 5 \text{ V}$ and $V_{GS} = 1 \text{ V}$. The result acquired through a wide range of frequencies 1 kHz to 1 THz. For the structure with B GaN back barrier, the results present that the peak value of these two parameters is about 115 dB. At 10 GHz, the GMA and GMS are 20 dB for the first structure and 25 dB for the second. It is improved compared to the HEMT without B GaN back barrier which displayed 110 dB. The result reveals a good stability performance shown by the device which make it appropriate for RF applications.

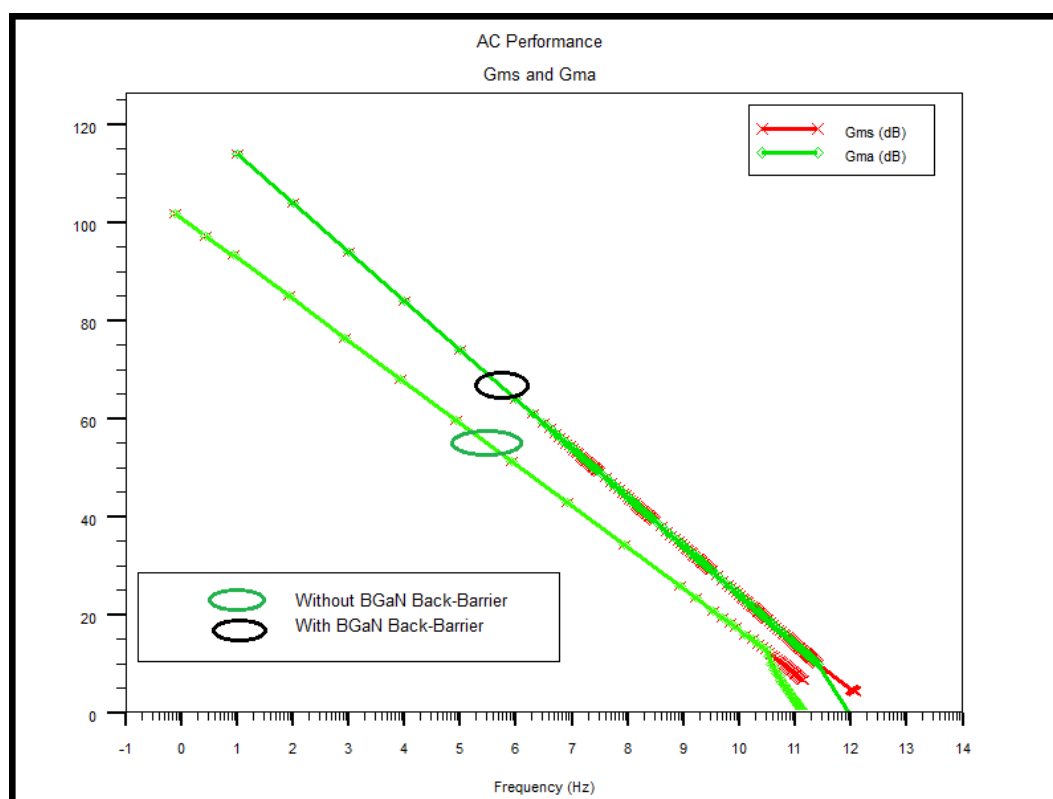


Figure 10. The simulated maximum gain power stability (GMS) and available maximum power gain (GMA) with $V_{DS}=5\text{ V}$ and $V_{GS}=1\text{ V}$

Table 3 summarizes a comparison of the major performances (maximum drain current, threshold voltage, transconductance, cut-off frequency, I_{ON}/I_{OFF} , DIBL and SS) calculated in this work for the structure with BgAn back barrier versus the results obtained by [22] [20] [21] [23] and [8].

From the results mentioned in Table 3, comparing our first work, HEMT without BgAn back barrier [8] and this work, it is figured out that the use of BgAn layer as back barriers utterly enhance the DC and AC performances of the high electron mobility transistor.

Table 3. Comparison of the performances of the propose device versus [22] [20] [21] [23] and [8].

	[22]	[20]	[21]	[23]	[8]	This work
ID (A/mm)	0.7	0.78	0.7	0.5	0.6	1
Vth (V)	-3.5	-3.6	-4.29	-3.9	-3.5	-1.25
Gate-leakage (A)	-	-	-	-	-	$5 \cdot 10^{-22}$
Ft (Ghz)	226	119	53.8	30	50	600
Fmax (Ghz)	277	300	82.4	100	150	1000
Gm (S/mm)	300	350	600	-	200	850
Ion/Ioff	$10^{8.7}$	$10^{9.4}$	10^{10}	-	10^9	$1.5 \cdot 10^9$
DIBL (mV/V)	-	-	53	-	22	166
SS (mV /dec)	-	-	134	-	200	300

4 CONCLUSION

We have discussed $\text{Al}_{0.26}\text{Ga}_{0.74}\text{N}/\text{GaN}/\text{B}_{0.02}\text{Ga}_{0.98}\text{N}/\text{HEMT}$ structures compared to the $\text{Al}_{0.26}\text{Ga}_{0.74}\text{N}/\text{GaN}$ HEMTs proposed in the first work [8] and other papers. The major purpose of this study was to ameliorate electron confinement and to prevent the leakage of electron for an AlGaIn/GaN HEMT structure by inducing a back barrier of BGaN beneath the channel. We obtained a maximum drain current of 1 A, a maximum transconductance of 850 mS/mm, and a high cut-off and maximum oscillation frequencies equal to 600 GHz and 1 THz, respectively. The obtained results show that the layer of $\text{B}_{0.02}\text{Ga}_{0.98}\text{N}$ as barrier of electrostatic which precludes the leakage of electron from the channel to the lower layers, as a consequence, improve the DC and AC characteristics. The splendid results obtained make the device highly attractive for future power electronics and switching applications.

REFERENCES

- [1] J. M. Barker and D. K. Ferry, "Bulk GaN and AlGaIn/GaN heterostructure drift velocity measurements and comparison to theoretical models," *Journal of Applied Physics*, vol. 97, no. 063705, 2005.
- [2] Y. S. Noh and I. B. Yom, "A linear GaN high power amplifier MMIC for Ka-band satellite communications," *IEEE Microw. Wireless Compon. Lett.*, vol. 26, no. 8, pp. 619–621, Aug. 2016.
- [3] R. J. Kaplar, A. A. Allerman, A. M. Armstrong, M. H. Crawford, J. R. Dickerson, A. J. Fischer, A. G. Baca and E. A. Douglas, "Ultra-Wide-Bandgap AlGaIn Power Electronic Devices," *ECS J. Solid State Sci. Techno*, vol. Q3061, 2017.
- [4] Jeremy R. Dickerson, Vinod Ravindran, Tarik Moudakir¹, Simon Gautier, Paul L. Voss, and Abdallah Ougazzaden, "A study of BGaN back-barriers for AlGaIn/GaN HEMTs" *Eur. Phys. J. Appl. Phys.* (2012) 60: 30101
- [5] A. Ougazzaden, S. Gautier, T. Moudakir, Z. Djebbour, Z. Lochner, S. Choi, H. J. Kim, J.-H. Ryou, R. D. Dupuis, and A. A. Sirenko, «Bandgap bowing in BGaN thin films,» *Applied Physics*, vol. 93, n° 083118, 2008
- [6] T. Baghdadli et al. Electrical and structural characterizations of BGaN thin films by metal-organic vapor phase epitaxy. *Phys. Status Sol. C*, 6 : S1029, 2009.
- [7] T. Akiyama, K. Nakamura, and T. Ito, "Effects of lattice constraint on structures and electronic properties of BAlN and BGaN alloys: A first-principles study", *Applied Physics Express* 11, 025501 (2018).
- [8] I. Four and M. Kameche "Optimization of DC and AC performances for $\text{Al}_{0.26}\text{Ga}_{0.74}\text{N}/\text{GaN}/4\text{H-SiC}$ HEMT with 30nm T-gate ", *International Journal of Nanoelectronics and Materials* Volume 13, No. 2, Apr 2020 [361-372]
- [9] F. Jabli, M. A. Zaidi, N. Ben Hamadi d, S. Althoyaib, M. Gassoumi, " Characterisation of the effect of surface passivation with SiO_2/SiN on deep levels in $\text{AlGaIn}/\text{GaN}/\text{Si}$ HEMTs," *Journal of Alloys and Compounds*, vol. 653, (2015)p. 624–628.
- [10] A.S. Augustine Fletcher, D. Nirmal, "A Survey of Gallium Nitrate HEMT for RF and High-Power application," *Superlattices and Microstructures*, vol. 38 (2017), pp. 2-3.
- [11] Jessen GH, Fitch RC, Gillespie JK, Via G, Crespo A, Langley D, et al. Short-channel effect limitations on high-frequency operation of AlGaIn/GaN HEMTs for T-Gate devices. *Electron Devices IEEE Trans* 2007 ;54 :2589–97.
- [12] D. B. S. Chowdhury, "Effect of device parameters on transmission coefficient of $\text{Al}_{0.2}\text{Ga}_{0.8}\text{N}/\text{GaN}$ Resonant Tunneling Diode grown on silicon substrate," *Nanoelectronics and Materials*, no. 6 pp.129-137, 2013.

- [13] Iwan Susanto, Ken-Yuan Kan and Ing-Song Yu " Temperature effects for GaN films grown on 4H-SiC substrate with miscutting orientation by plasma-assisted molecular beam epitaxy" HYPERLINK "<https://www.sciencedirect.com/science/journal/09258388/723/supp/C>" \o "Go to table of contents for this volume/issue" Vol 723, 5 November 2017, Pages 21-29.
- [14] O. Ambacher, J. A. Majewski, C. Miskys, A. Link, M. Hermann, M. Eickhoff, M. Stutzmann, F. Bernardini, V. Fiorentini, V. Tilak, B. Schaff, and L. F. Eastman, "Pyroelectric properties of Al (In)GaN/GaN hetero- and quantum well structures," J. Phys.: Condens. Matter 14, 3399 (2002).
- [15] I. Silvaco, Silvaco Atlas User Manual, 2016, <http://www.silvaco.com/>
- [16] Piprek J. Semiconductor optoelectronic devices: introduction to physics and simulation. UCSB : Academic Press; 2003. p. 22.
- [17] Azzi S, Zaoui A, Ferhat M. On the importance of the band gap bowing in Boronbased III-V ternary alloys. Solid State Commun 2007; 144:245–8.
- [18] O. Ambacher, B. Foutz, J. Smart, J. R. Shealy, N. G. Weimann, K. Chu, M. Murphy, A. J. Sierakowski, W. J. Schaff, and L. F. Eastman, "Two dimensional electron gases induced by spontaneous and piezoelectric polarization in undoped and doped AlGaIn/GaN heterostructures," Appl. Phys., vol. 334, no. 87, 2000
- [19] Vurgaftman I, Meyer JR, Ram-Mohan LR. Band parameters for III-V compound semiconductors and their alloys. J Appl Phys 2001;89(11):5815–75.
- [20] Lotfi Guenineche and Abdelkader Hamdoune, "Influence of a BGaN back-barrier on DC and dynamic performances of an AlGaIn/GaN HEMT: simulation study"; Materials Research Express, Volume 3, Number 5, Published 29 April 2016.
- [21] Remzi Yildirim, Huseyin Guçlu Yavuzcan, Levent Gokrem, Technology 12, 201 (2009).
- [22] L. Guenineche, A. Hamdoune, "Improvement of DC and RF Performances of an AlGaIn/GaN HEMT by a B_{0.01}Ga_{0.99}N Back-Barrier Simulation Study," in THE 9th INTERNATIONAL SYMPOSIUM ON ADVANCED TOPICS IN ELECTRICAL ENGINEERING, Bucharest, Romania, 2015.
- [23] Moujahed GASSOUMI, Abdelhamid HELALI, Hassen MAAREF, Malek GASSOUMI, " DC and RF characteristics optimization of AlGaIn/GaN/BGaN/GaN/Si HEMT for microwave-power and high temperature application" Journal of Results in Physics Vol 12, (2019) p. 302–306.